Simulation of fracture behaviour of hydrogel by discrete element method

Runhuai Yang[1,*] ✉, *Tianyun Gao*[1,*], *Didi Li*[1], *Haiyi Liang*[2,3], *Qingqing Xu*[4]

[1]*Department of Biomedical Engineering, School of Life Science, Anhui Medical University, 230032 Hefei, People's Republic of China*
[2]*CAS Key Laboratory of Mechanical Behavior and Design of Materials, University of Science and Technology of China, 230027 Hefei, People's Republic of China*
[3]*IAT-Chungu Joint Laboratory for Additive Manufacturing, Institute of Advanced Technology, University of Science and Technology of China, 230026 Hefei, People's Republic of China*
[4]*The First Clinical Medical College, Anhui Medical University, 230032 Hefei, People's Republic of China*
[*]*Runhuai Yang and Tianyun Gao contributed equally to this work.*
✉ *E-mail: yangrunhuai@ahmu.edu.cn*

Published in Micro & Nano Letters; Received on 25th November 2017; Revised on 16th January 2018; Accepted on 9th February 2018

The determination of fracture properties of hydrogels is of great importance while the hydrogel is used as medical scaffold or soft robotic. The simulations of the mechanical properties were used to reduce the experiment cost and improve efficiency. Here, the work presents a novel method to simulate the fracture behaviour of hydrogels based on discrete element method. Different with continuous methods, the hydrogel was characterised by number of particles. The viscoelastic model and bonding model within the particle model were applied to simulate the microscopic structure of hydrogels. By changing the critical parameters in the model, hydrogels with different mechanical properties were also simulated. Puncture compression test and uniaxial tensile test based on the model were performed. The fracture morphology, stress and strain during the tests were simulated. The results show that the model provides a novel and effective tool to simulate the fracture process of hydrogels.

1. Introduction: Hydrogels are promising functional biomaterials which were recently used as a biological scaffold and soft robotics [1]. The low cost, wide availability and high biocompatibility have led to a continually increasing usage in the bio-medical and material field [2]. Multifunctional hydrogels were developed [3, 4] so that the hydrogels were considered as smart materials for controllable medical micromachines. Since hydrogels are frequently used as scaffolds [5] or as the actuator of soft robotic [6] in medical applications, the determination of the fracture behaviour is of great importance to avoid a medical accident such as the hydrogels could be broken in human body. The ability of hydrogels to sustain a load without undue deformation or failure should be precisely studied.

Physical and chemical interactions within hydrogels play a key role in the mechanical properties [7]. This led to complicated processes in fracture formation and development. Therefore, the fracture properties were mostly studied by experiments such as puncture, uniaxial compression and wire cutting methods [8]. Recently, the increasing use of simulation tools for studying the materials properties reduced the experiment cost and improves efficiency. However, the simulation of the fracture properties of hydrogels is not a simple task. Hydrogels have wide range modulus (from the order of $1–1\times10^{100}$ kPa) which is quite lower than the traditional materials that are widely studied [7]. Besides, the hydrogels support large deformations and present the hyperelastic behaviours [9]. The width of the fracture area of hydrogels can be sizable. Therefore, the continuum model is not suitable for the simulation of the fracture of hydrogels.

Discrete element method (DEM) considers the materials as separable solid particles. Compared to the continuum model, DEM provides an easy way to study the fracture behaviour under large deformations and sizable crack. The model could also directly simulate the morphology before and after fracture [10]. However, DEM is frequently used to solve problems in rock and soil mechanics [11], concrete [12] etc. The swollen properties of hydrogel were studied. However, the application of DEM to simulate the mechanical properties of hydrogels which support large deformations and strain hardening was seldom reported. In the present Letter, DEM was modified and applied to simulate the fraction test for hydrogels.

2. Model: Fig. 1 shows the illustration of the microscopic structure of hydrogel and the discrete element model of the hydrogel. As shown in Fig. 1*a*, hydrogels are network polymeric materials, which have the cross-links at the intersection points of polymer chains or have physical entanglements between polymer chains generating cohesive forces. Besides, hydrogels are filled with large quantities of water and show hyperelastic properties. To simulate the mechanical properties of hydrogels, a 'particle model' which consists of stiffness model, viscoelastic model and bonding model was adopted in our simulation. The stiffness model is defined by the normal and shear stiffness, K_n and K_s, as shown in Fig. 1*b*. The index '*n*' presents the parameter in normal direction and '*s*' presents the parameter in the shear direction. The normal stiffness was defined by the normal force divided by normal displacement, and the shear stiffness related the increment of shear force to the shear displacement. The normal stiffness was considered as two sub-springs. Considering the normal force and the moment, in each Δt the normal force was calculated as follows for each spring:

$$\begin{aligned}\Delta F_n &= \frac{1}{2}K_n v_n \Delta t \pm \frac{1}{4}\dot{\theta}_{ij}\Delta t l_k K_n,\\ F_n^t &= F_n^{t-\Delta t} + \Delta F_n\end{aligned} \tag{1}$$

where v_n presents the normal velocity of the two particles and $\dot{\theta}_{ij}$ presents the relative angular velocity, l_k presents the distance between the two normal springs.

The shear force was calculated as follows:

$$\begin{aligned}\Delta F_s &= K_s v_s \Delta t,\\ F_s^t &= F_n^{t-\Delta t} + \Delta F_n\end{aligned} \tag{2}$$

where v_n presents the shear velocity of the two particles.

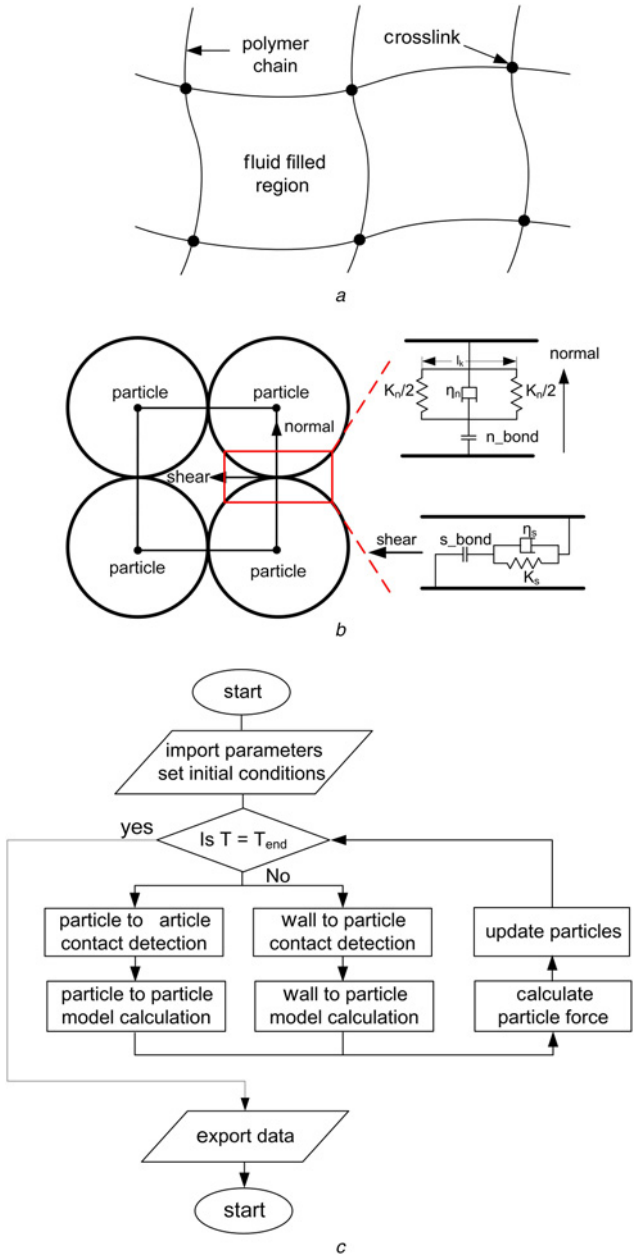

Fig. 1 *Microscopic structure of hydrogel and the DEM model for hydrogel*
a Illustration of the microscopic structure of the hydrogel
b Discrete element model for hydrogel, where the n_bond presents the normal bond, s_bond presents the shear bond, K_n presents the normal stiffness, K_s presents the shear stiffness, V_n and V_s present the normal and shear viscosity
c Diagram showing the DEM programme structure

The viscoelastic model was also applied, which was presented as the normal viscosity η_n and shear viscosity η_s. Therefore, the normal and shear contact consist of a spring in series with a dashpot. The viscous force was expressed as follows:

$$F_s^{vs} = \eta_s K_s v_s, \quad F_n^{vs} = \eta_n K_n v_n \tag{3}$$

After the force was calculated, the particle's states including velocity, acceleration and position were updated according to Newton's second law of motion. To simulate the fracture properties, bonding models were applied to every particle in normal and shear contacts. The bonds were a kind of glue joining the two particles and bind the particles together. If the magnitude of the contact force exceeded the bond strength, the bond would be broken. The bond was used to simulate the cross-link and cohesion force of hydrogels. n_bond presents a tension strength which bonds the particles together on the normal direction of the particles. The contact bond is initially formed, and it will be broken when the normal force is higher than the tension strength. Therefore, the bond on normal direction will be broken when the following conditions are satisfied:

$$F_n \geq \text{n\_bond} \tag{4}$$

Considering the friction of hydrogel, the shear bond will be broken when the following conditions are satisfied:

$$F_s \geq F_n \tan \varphi + \text{s\_bond} \tag{5}$$

where φ presents the friction angle.

To accomplish the puncture test and the tensile test, the 'wall model' was adopted to simulate the substrate, clamp and the punch. Common materials used for the substrate and punch are polymethylmethacrylate and teflon. Therefore, the 'wall model' has the stiffness model and bond model, and friction between the 'particle model' and the 'wall model' was considered. The algorithms of the calculation are shown in Fig. 1*c*. In each step, the data of particles and walls were updated. Contact detection of particles and walls was conducted. Force for each particle was calculated from the particle position and the models. The stiffness model, viscoelastic model and bonding model are used to calculate the force–deformation relationship between particles. All of these calculations were built up by using a common programming environment with graphical user interface (MATLAB 7.0).

3. Simulation and results of puncture experiment: A flat-faced punch used in the puncture experiment was pushed into the

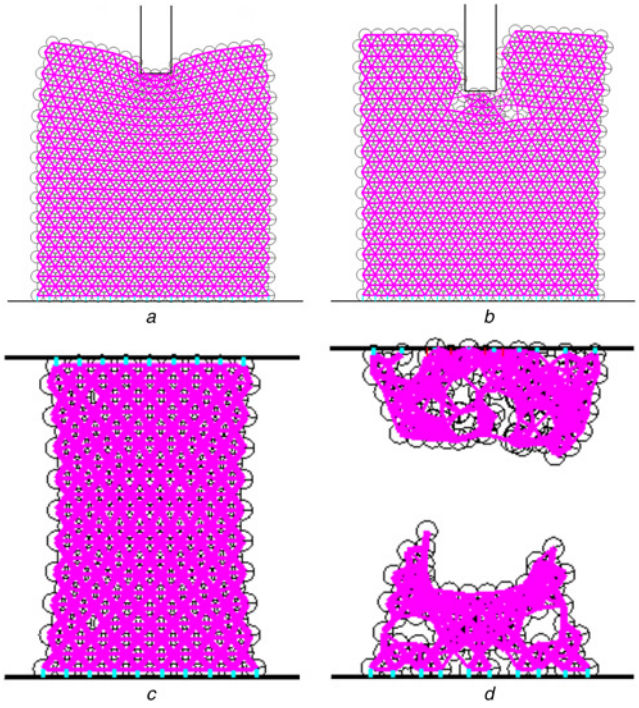

Fig. 2 *Morphology of the hydrogel sample before and after the fracture behaviour*
a Hydrogel in puncture test before fracture
b Hydrogel in puncture test after fracture
c Hydrogel in tensile test before fracture
d Hydrogel in tensile test after fracture

doi: 10.1049/mnl.2017.0844

hydrogel samples, and the fracture displacement and strain energy could be recorded. The strength of deferent hydrogels could be recorded and compared by the tests [13]. In our simulations, the puncture tests were performed by a flat-faced punch (10 mm diameter) toward a hydrogel sample of 80 mm height and 60 mm diameter a hydrogel sample was built up by particle model, and a punch was built up by the wall model, as shown in Fig. 3*a*. The white circle is the particle model, while the pink line shows the connecting bond between each particle. After the hydrogel sample was built up, the bond was generated between each particle to simulate the cohesion effect in hydrogels. Besides, a uniaxial tensile test was also performed by our simulations, as shown in Fig. 3*b*. The 'wall model' was used as the rigid clamp. The blue line presents the bond between wall and particles.

The change of the morphology during the simulation was captured, as shown in Fig. 2. Fig. 2*a* shows the deformation of hydrogel sample before the fracture happened. It is obvious that a large deformation happened near the punch area which was similar to the reported experimental results [10]. Fig. 2*b* shows the crack near the punch after the fracture happened. Similarly, Figs. 2*c* and *d* show the morphology of the hydrogel in a tensile test. The results of the puncture test show that the morphology of the hydrogel sample during the simulation is similar to the experimental study.

In puncture test, the normal stress–displacement or force–displacement curve can be recorded and the fracture properties can be studied [14]. To verify, the model can be used to simulate hydrogels with different mechanical properties, two hydrogel samples were simulated in the puncture test. The parameters for 'high cross-link hydrogel' were as follows: normal stiffness (K_n) was set as 0.9×10^4 N/m, the shear stiffness (K_s) was set as 0.9×10^4 N/m, the n_bond was set to 0.9×10^4 N/m, s_bond was 0.9×10^4 N/m, and viscous coefficient (η_n *and* η_s) was 0.01. The parameters for 'low cross-link hydrogel' is as follows: normal stiffness (K_n) was set as 0.45×10^4 N/m, the shear stiffness (K_s) was set as 0.45×10^4 N/m, the n_bond was set as 0.3×10^4 N/m, s_bond was 0.3×10^4 N/m, and viscous coefficient (η_n *and* η_s) was 0.01. Fig. 4 shows the normal stress and the strain energy curves obtained by DEM. As can been seen from the curves, the curves show the fluctuation of normal stress and strain energy, and the black arrows indicate the fracture point. For the curve of high cross-link hydrogel, a peak corresponding to the initial fracture is observed, followed by the highest peak caused by final fracture. The low cross-link hydrogel has smoother force–distance curves. The highest normal force was considered as the fracture point in the puncture test. After the punch obtained the highest normal force, the force curve significantly declined, showing that the structure of hydrogel was fractured and lost the capability to support the

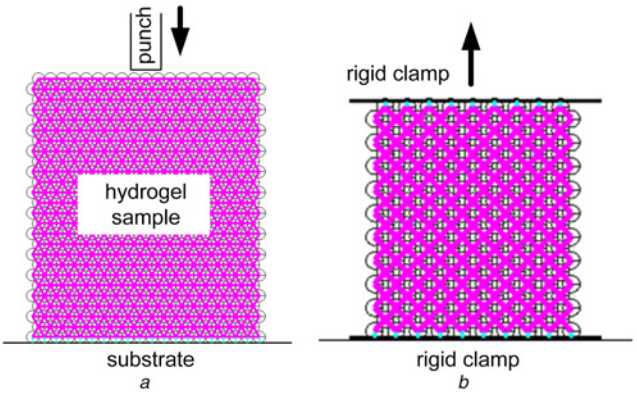

Fig. 3 *Schematic representation of the initial state*
a Puncture test
b Uniaxial tensile test

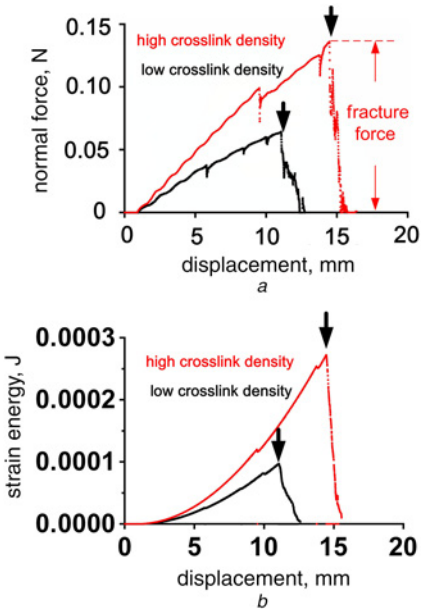

Fig. 4 *Results of puncture test by DEM simulation*
a Stress–displacement curve of puncture test
b Strain energy–displacement curves of hydrogel

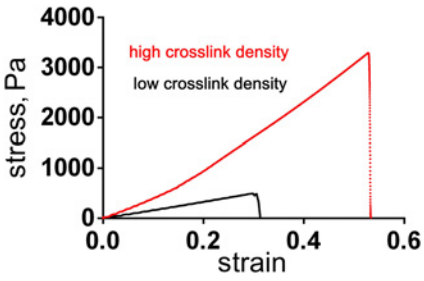

Fig. 5 *Stress–strain curve of tensile test*

punch. The two curves show that the high cross-link hydrogel increased faster, and it took a longer distance to fracture the hydrogel, indicating that the high cross-link hydrogel is stronger than the low cross-link hydrogel. After the fracture displacement, a considerable decrease occurred and the strain energy suddenly dropped to nearly zero. Experimental study of puncture test could obtain two critical results: fracture force and fracture distance for different samples [15]. In our simulation results, the curves for low and high cross-link density hydrogels were obtained, and the fracture force and fracture distance were obtained by the curves. Compared to the low cross-link density hydrogel, the high cross-link density hydrogel had a higher fracture force and fracture distance, which was similar to the experimental study.

Similarly, the tensile tests were performed for two types of hydrogel samples. Typical stress–strain curves were obtained for hydrogel samples, as shown in Fig. 5. The hydrogel sample with low cross-link density fractured after strain = 0.3, while the hydrogel sample with high cross-link density fractured after strain>0.6. The slopes of the two curves also show that the high cross-linked hydrogel has a higher modulus than low cross-linked hydrogel. The simulation results of tensile tests demonstrate that hydrogels with different tensile strength and large deformation (>0.5) can be simulated by our model.

4. Conclusion: In summary, a mechanical model for hydrogel based on the DEM was developed to investigate the fracture

properties of hydrogels. The cohesion and viscoelastic effects of hydrogels were considered and simulated by the model. A puncture test was performed by the model to simulate the fracture behaviour. The hydrogel sample was characterised by the particle model and the punch and substrate were characterised by the wall model. The results of the puncture test show that the morphology of the hydrogel samples during the simulation is similar to the experimental study. Besides, two types of hydrogel sample were simulated, and typical strain energy curve was obtained indicating that the model was suitable for the simulation of the fracture test. The results show that this method will improve the simulation of the fracture behaviour of hydrogels. In future work, a calibration process will be further studied to precisely determine the parameters between particles by mimicking the actual physical test.

5. Acknowledgments: This work was supported by the National Natural Science Foundation of China (grant no. 61603002), the Scientific Research of BSKY (grant no. XJ201517) from Anhui Medical University, and Fundamental Research Funds for the Central Universities of China (grant nos.WK2480000001, WK2090050040).

6 References

[1] Kim S., Laschi C., Trimmer B.: 'Soft robotics: a bioinspired evolution in robotics', *Trends in Biotechnology*, 2013, **31**, pp. 287–294
[2] Tibbitt M.W., Anseth K.S.: 'Hydrogels as extracellular matrix mimics for 3D cell culture', 2009, **103**, pp. 655–663
[3] Huang H.W., Sakar M.S., Petruska A.J., *ET AL.*: 'Soft micromachines with programmable motility and morphology', *Nat. Commun.*, 2016, **7**, p. 12263
[4] Palleau E., Morales D., Dickey M.D., *ET AL.*: 'Reversible patterning and actuation of hydrogels by electrically assisted ionoprinting', *Nat. Commun.*, 2013, **4**, p. 2257
[5] Ni Y., Tang Z., Cao W., *ET AL.*: 'Tough and elastic hydrogel of hyaluronic acid and chondroitin sulfate as potential cell scaffold materials', *Int. J. Biol. Macromol.*, 2015, **74**, pp. 367–375
[6] Zolfagharian A., Kouzani A.Z., Khoo S.Y., *ET AL.*: 'Development and analysis of a 3D printed hydrogel soft actuator', *Sens. Actuators A, Phys.*, 2017, **265**, pp. 94–101
[7] Oyen M.L.: 'Mechanical characterisation of hydrogel materials', *Int. Mater. Rev.*, 2014, **59**, (1), pp. 44–59
[8] Czerner M., Fasce L.A., Martucci J.F., *ET AL.*: 'Deformation and fracture behavior of physical gelatin gel systems', *Food Hydrocolloids*, 2016, **60**, pp. 299–307
[9] Sun J.-Y., Zhao X., Illeperuma W.R.K., *ET AL.*: 'Highly stretchable and tough hydrogels', *Nature*, 2012, **489**, (7414), pp. 133–136
[10] Abbasnia1 R., Aslami M.: 'Numerical simulation of concrete fracture under compression by explicit discrete element method', *Int. J. Civ. Eng.*, 2015, **13**, (3), pp. 245–254
[11] Donzé F.V., Richefeu V., Magnier S.-A.: 'Advances in discrete element method applied to soil, rock and concrete mechanics', *Electron. J. Geotech. Eng.*, 2009, **8**, pp. 1–44
[12] Tran V.T., Donzé F.V., Marin P.: 'A discrete element model of concrete under high triaxial loading', *Cement Concrete Compos.*, 2011, **33**, pp. 936–948
[13] Sanchez Fellay L., Fasce L.A., Czerner M., *ET AL.*: 'On the feasibility of identifying first order Ogden constitutive parameters of gelatin gels from flat punch indentation tests', *Soft Mater.*, 2015, **13**, (4), pp. 188–200
[14] Chiou B.-S., Avena-Bustillos R.J., Shey J., *ET AL.*: 'Rheological and mechanical properties of cross-linked fish gelatins', *Polymer (Guildf)*, 2006, **47**, (18), pp. 6379–6386
[15] Hayakawa F., Kazami Y., Ishihara S., *ET AL.*: 'Characterization of eating difficulty by sensory evaluation of hydrocolloid gels', *Food Hydrocolloids*, 2014, **38**, pp. 95–103

doi: 10.1049/mnl.2017.0844